Investigation of Patient Positioning Accuracy in

Lung Stereotactic Body Radiation Therapy

by

Kathryn Rachel Turner

Graduate Program in Medical Physics
Duke University

Date:_______________________
Approved:

____
Jing Cai, Supervisor

____
Fang-Fang Yin, Chair

____
William Paul Segars

Thesis submitted in partial fulfillment of
the requirements for the degree of Master of Science in the
Graduate Program in Medical Physics
in the Graduate School
of Duke University

2013

ABSTRACT

Investigation of Patient Positioning Accuracy in

Lung Stereotactic Body Radiation Therapy

by

Kathryn Rachel Turner

Graduate Program in Medical Physics
Duke University

Date:_______________________
Approved:

____
Jing Cai, Supervisor

____
Fang-Fang Yin, Chair

____
William Paul Segars

An abstract of a thesis submitted in partial fulfillment of
the requirements for the degree of Master of Science in the
Graduate Program in Medical Physics
in the Graduate School of
Duke University

2013

Abstract

Purpose: It has been shown that patients' irregular breathing can cause variation in the delineation of the internal target volume (ITV) and affect the accuracy of four dimensional computed tomography (4DCT) and cone-beam computed tomography (CBCT) images. Therefore, it is expected that the variations induced by irregular breathing will also affect image registration between the two images. This study aims to quantitatively assess breathing irregularity induced error in CBCT-based target localization in lung stereotactic body radiation therapy (SBRT) and correlate the error with a measure of breathing variability.

Methods and Materials: For examining methods of ITV delineation, the Computerized Imaging Reference Systems (CIRS) Dynamic Thorax Phantom Model 008A (CIRS, Norfolk, VA) with CIRS motion control software was used to model 4 irregular patient respiratory profiles and one regular respiratory profile (sine wave) with a 3 cm tumor insert. A 3D-CT and repeated 4D-CT scans were performed on a 4-slice clinical scanner (Lightspeed, GE, WI). The RPM system (Varian, Palo Alto, CA) was used to track the respiratory profiles. V was contoured on 3D-CT, and ITV was contoured on each MIP (ITV_{MIP}) using a consistent lung window by the same person. The new method of creating ITV was to combine the V and ITV_{MIP}, namely ITV_{COMB}. To evaluate which ITV is more accurate, ITV_{COMB} and ITV_{MIP} were compared to a "reference standard" ITV (ITV_{RS}) which was generated by combining the three ITV_{MIPs}. To investigate the error in image registration between the CBCT and 4DCT, the 4D extended cardiac-torso (XCAT) digital phantom was used to generate 10-phase 4DCTand CBCT images using in-house

developed simulation programs. Images were generated using the same clinical-based parameters for various respiratory profiles (one regular sinusoidal and 10 irregular) and tumor sizes (1 cm, 2 cm, 3 cm). Maximum intensity projection (MIP) and average intensity projection (AIP) images were generated from 4DCT images The ITVs were contoured by the same user with the same window/level in Eclipse. Image registrations were performed between CBCT and AIP images by matching the target as in the clinic, for each respiratory profile and tumor size. Error of registration was determined as the difference between the manual CBCT-to-AIP registration and the known registration between the two. Variability of the respiratory profiles was measured, and a correlation between the error and breathing irregularity was investigated. Additionally, variation in ITV volumes among AIP, MIP, and CBCT images were examined.

Results: When examining the volumes for the ITV delineation study, for the regular profile, both ITV_{MIP} (27.25 cm^3) and ITV_{COMB} (28.12cm^3) were comparable to ITV_{RS} (27.25 cm^3). For irregular profiles, the mean difference between ITV_{COMB} and ITV_{RS} (6.3%±4.9) was significantly (p-value=0.0078) smaller than that between ITV_{MIP} and ITV_{RS} (18.1%±12.3). A total of 33 registrations were performed to investigate error in image registration. As expected, negligible errors of registration were found for the regular respiratory profile at all tumor sizes: the median (± SD) error was 0.50 (± 0.73) mm, 0.20 (± 0.17) mm, and 0.40 (± 0.22) mm in the medial-lateral (ML), anterior-posterior (AP), and superior-inferior (SI) direction, respectively. For the irregular respiratory profiles and all tumor sizes combined, maximum average error of registration was 1.0 mm, 2.0 mm, and 5.4 mm in the ML, AP, and SI direction, respectively. Median errors were

found small in ML and AP directions (the median (± SD) error was 0.50 (± 0.21) mm and 0.50 (± 0.71) mm respectively), primarily due to small motion in these two directions. Median error in the SI direction was found non-trivial (the median (± SD) error was 1.90 (± 1.55) mm).

Conclusions: The results suggest that combining GTV of the 3D-CT with the ITV of the MIP is more accurate than the ITV of the MIP alone, and thus would be a simple method to reduce breathing irregularity induced errors in ITV delineation for treatment planning of lung cancer. Errors could occur during CBCT-to-AIP registration in lung SBRT when patient's breathing is irregular, especially in the SI direction. The error is largely induced by breathing irregularity and could not be overcome by perfecting manual matching, and it should be considered when determining the ITV to PTV margin. Differences in ITV volumes for AIP-MIP were seen to be minimal. However, significant differences in ITV volumes for MIP-CBCT were observed. Further studies of clinically minimizing such uncertainties are desirable.

Contents

Abstract......iv

List of Tables......ix

List of Figures......x

List of Abbreviations......xii

Acknowledgements......xiii

1. Introduction......1

    1.1 Potential problems with 4DCT and CBCT......1

    1.2 Delineation of the Internal Target Volume......2

    1.3 Purpose of this study......4

2. Methods and Materials......5

    2.1 Minimizing error in ITV delineation: a phantom study......5

      2.1.1 Data generation......5

      2.1.2 Contouring and development of new ITV method......7

      2.1.3 Data Analysis......8

    2.2 Uncertainties in target localization in lung SBRT......8

      2.2.1 The XCAT Phantom......9

      2.2.2 Data generation......12

        2.2.2.1 4DCT Parameters......14

        2.2.2.2 CBCT Parameters......15

      2.2.3 Contouring......16

      2.2.4 Image Registration......16

      2.2.5 Data Analysis......18

    2.3 Examining differences in ITV delineation for MIP, AIP, and CBCT......18

3.1 Uncertainties in 4DCT-based ITV delineation 20
3.2 Target localization accuracy in lung SBRT 22
3.2.1 Overall results observed for target localization error 22
3.2.2 Difference in error among different tumor size groups 23
3.2.3 Correlation between error in the S/I direction and respiratory variability 24
3.2.4 Correlation between error in the S/I direction and I/E ratio 26
3.3 Differences in ITV for MIP, AIP, and CBCT 28
4. Discussion 31
4.1 Limitations of this study 31
4.2 Clinical impact 32
4.3 Other relevant studies 34
5. Conclusion 36
Appendix A: Illustrations of RPM respiratory trajectories 37
References 39

List of Tables

Table 1: Characteristics of respiratory profiles used to generate 4DCT and CBCT data.. 14

Table 2: I/E ratios for respiratory profiles 27

Table 3: Average percent error for ITV delineation methods among different tumor size groups 30

List of Figures

Figure 1: Schematic of the boundaries of target volumes, courtesy of ICRU Report 62.... 3

Figure 2: CIRS dynamic thorax phantom used to model respiratory trajectories. 6

Figure 3: Diagram demonstrating the new process of ITV delineation 8

Figure 4: Schematic illustrating overall workflow for the study... 9

Figure 5: Anterior views of the 4D-XCAT phantoms. (Male- left, Female- right) Illustration courtesy of Dr. William Paul Segars. 10

Figure 6: Comparison of input and measured respiratory trajectories. 12

Figure 7: 4D-XCAT graphical user interface used to generate images............................... 13

Figure 8: Image illustrating 10-phase 4DCT generated using the 4D-XCAT phantom 15

Figure 9: Example of CBCT generated using the 4D-XCAT phantom. 16

Figure 10: Screenshot illustrating image registration between the AIP (left) and CBCT (right) based on target volume matching. 17

Figure 11: Screenshot illustrating ITV contours for the AIP (red), CBCT (blue), and MIP (green). 19

Figure 12: Comparison of ITV volumes to the reference standard as delineated by the typical MIP-based method and the new MIP and GTV-based method. Profiles #1-4 are irregular, and profile #5 is a regular sinusoidal curve. 21

Figure 13: Variation in ITV from three randomly generated 4DCTs for irregular respiratory profiles. 21

Figure 14: Boxplot of image registration errors for various respiratory trajectories. 23

Figure 15: Illustration of error in image registration among different tumor size groups. 24

Figure 16: Plots demonstrating correlation between breathing variability in respiratory trajectory and median error in CBCT-to-AIP image registration for all tumor sizes and for each tumor size separately. 25

Figure 17: Comparison of median error in the SI direction for low vs. high variability respiratory trajectories for all tumor sizes and individual groups 26

Figure 18: Correlation between SI registration error and inspiration to expiration ratio 27

Figure 19: Plots demonstrating difference in volumes of MIP, AIP, and CBCT-based ITV delineation for 1 cm, 2 cm, and 3 cm tumors. 29

List of Abbreviations

- 4D XCAT- four dimensional extended cardiac-torso (XCAT) digital phantom
- 4DCT- four dimensional computed tomography
- AIP- average intensity projection
- ANOVA- analysis of variance
- AP- anterior/posterior
- CBCT- cone beam computed tomography
- GTV- gross tumor volume
- ITV- internal target volume
- MIP- maximum intensity projection
- ML- medial/lateral
- PTV- planning target volume
- RPM- real time position management
- SBRT- stereotactic body radiation therapy
- SD- standard deviation
- SI- superior/inferior

Acknowledgements

I would like to thank my advisor, Dr. Jing Cai, for his time and support throughout my work on this project and Dr. Fang-Fang Yin and Dr. Paul Segars for serving on my committee and offering their advice and expertise. I would also like to acknowledge Dr. Lei Ren and physicians Dr. David Yoo and Dr. Christopher Kelsey for performing image registrations for my project. Additionally, I would like to thank the other medical physics students in the lab for assistance with my project: Irina Vergalasova, You Zhang, and Hao Li.

1. Introduction

With more people in the United States dying from lung cancer than any other cancer, research for effective treatment techniques has become increasingly important. (1) Stereotactic body radiation therapy (SBRT), which delivers a high dose per fraction for a small number of fractions, has proven to be a promising technique for the treatment of early-stage non-small cell lung cancer (NSCLC) and or oligometastatic lesions to the lung. Studies have shown good tumor control and have the advantage of a more convenient, shorter treatment time for the patient. (2-4) Along with the higher dose per fraction in SBRT treatments comes the emphasis on treatment accuracy, especially respiratory motion tracking, the delineation of the internal target volume (ITV) and accurate target localization. (5) Respiratory motion, often irregular, poses great challenges for lung SBRT treatment. If not properly managed, it may cause errors in target volume delineation and target localization, leading to compromised efficacy of the lung SBRT treatment.

1.1 Potential problems with 4DCT and CBCT

For contouring the ITV, which will be further described below, a four-dimensional computed tomography (4DCT) scan is the typical protocol for lung SBRT treatments. A 4DCT essentially acquires several CT images per slice to capture the motion due to breathing and sorts the datasets into phases. Typically, data is binned into 10 phases, with 0% as peak inspiration and 50% as peak expiration. (6) While 4DCT has become the clinical standard for tumor motion measurement and target volume determination, there still are several issues with 4DCT that need to be resolved. The current 4DCT methods lead to artifacts during image acquisition and reconstruction due mismatched phase between CT slices and displacement between couch positions. Yamamoto et. al. conducted a retrospective study of 50 thoracic 4DCT patients and analyzed artifacts including, blurring, duplicate structure, and overlapping structure. Their findings indicated that 90% of patients had at least one 4DCT artifact other than blurring. (7) Additionally, studies have shown that artifacts induced by phase assignment errors increase with larger motion amplitudes, smaller tumor volumes, and especially with respiratory irregularity. (8, 9)

For daily localization, CBCT is used for lung SBRT cases. Similarly, CBCT is also affected by breathing irregularity. Because of the slow gantry rotation speed, CBCT is prone to imaging artifacts such as blurring and streaking, which make delineating the shape and size of the target volume more difficult. The existence of these artifacts is only worsened by respiratory motion, especially for irregular breathing patterns. Developments in four dimensional cone beam computed tomography (4D-CBCT) technology are working to eliminate and reduce breathing-induced CBCT artifacts. (10, 11)

1.2 Delineation of the Internal Target Volume

According to the International Commission on Radiation Units and Measurements report 62, the ITV should include all positions of the target volume throughout the respiratory cycle, as defined by the schematic below.

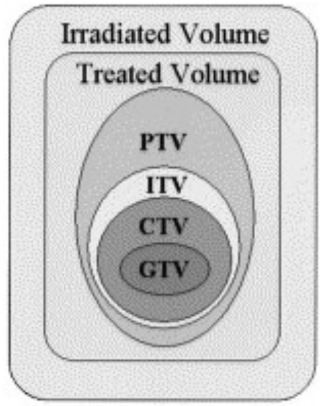

Figure 1: Schematic of the boundaries of target volumes, courtesy of ICRU Report 62

However, irregular respiratory trajectories induce error into the delineation of the ITV. The ITV is most often determined clinically using the maximum intensity projection (MIP) of the 4DCT. The MIP takes the maximum pixel value for each tumor position during the respiratory cycle and effectively combines these pixel values into a composite image. For regular respiratory trajectories, this method has proven to be accurate, but for irregular respiratory trajectories errors are induced. James et al. found variations in the ITV by simulating actual patient respiratory trajectories for 10, 20, and 3 mm tumor models. Differences in the ITV averaged from 12-27% for a 10 mm diameter tumor, 6%-99% for a 20 mm diameter tumor, and 15-69% for a 30 mm diameter tumor. (12) From this data, it can be seen that respiratory motion has a major impact on ITV delineation.

Additionally, the ITV can be delineated on the CBCT to assist with image registration. When delineating the ITV on the CBCT, poor image quality poses a problem. Motion-induced artifacts and blurriness make it difficult to clearly delineate the target, and studies have shown that ITVs delineated on the CBCT underestimate tumor volume. Liu et al. found that in comparison to the 4DCT-based ITV, the CBCT-based ITV was smaller on average by 11.8% ($p<0.01$). (13) Similarly, Vergalasova et al. found underestimations in the ITV delineated on the CBCT by 24.2% and 40.1%, for a large and small tumor, respectively. (14)

1.3 Purpose of this study

For lung SBRT treatments, a clinical planning process involved contouring the ITV on the MIP and copying the ITV to the AIP generated from the 4DCT. The treatment is planned on the AIP, and daily localization is performed using CBCT. When taking into account the respective errors of ITV delineation from the 4DCT and the daily setup using FB-CBCT for irregular respiratory trajectories, it can be hypothesized that image registration will ultimately induce further errors in ITV alignment and eventually dose deliver. In this study, the variation in 4DCT based ITV delineation will be examined with a focus on MIP-based ITV underestimations.

Additionally, the overall effects of irregular respiratory trajectories on matching the ITV from the 4DCT to the daily setup FB-CBCT will be examined, and the difference in volume between ITV delineation on AIP, MIP, and CBCT will be compared.

2. Methods and Materials

This study involves examining error in target localization for lung SBRT treatments. Error in MIP-based ITV delineation for treatment planning will be examined, and difference volumes generated from MIP, AIP, and CBCT will be compared. It can be inferred that the errors in ITV delineation will be carried further through the treatment planning process and can affect daily image registration. This concept will be further investigated by determining the error in daily image registration between AIP and CBCT images. The affect of both regular and irregular respiratory trajectories will be considered on ITV delineation and image registration.

2.1 Minimizing error in ITV delineation: a phantom study

As previously mentioned, the ITV is typically delineated on the MIP in the clinic. For regular breathing, this method proves to be effective, but for irregular breathing, variation in the delineation of the ITV can be observed. Previous studies have shown that MIP-based ITV can underestimate true tumor range.(14) This study examines a simple method to reduce such errors by combining the GTV of 3D-CT with the ITV of MIP.

2.1.1 Data generation

To investigate the error in typical ITV delineation, the Computerized Imaging Reference Systems (CIRS) Dynamic Thorax Phantom Model 008A (CIRS, Norfolk, VA) with CIRS motion control software was used to model 4 irregular patient respiratory trajectory and one regular respiratory trajectory (a sinusoidal curve). The CIRS phantom is an average human thorax containing a lung-equivalent rod with a spherical tumor insert. A motor is connected to the body of the phantom and translates and rotates the rod in the phantom to model three-dimensional tumor motion.

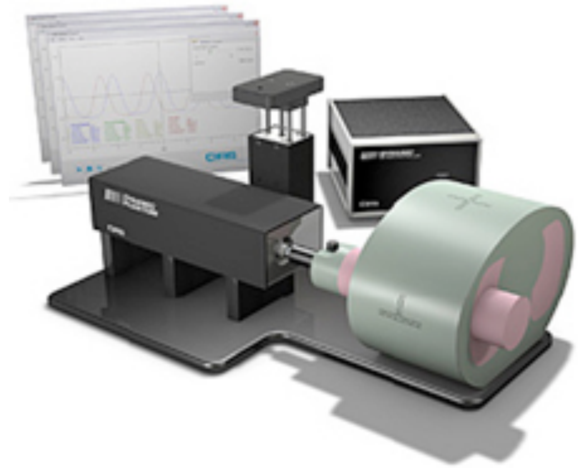

Figure 2: CIRS dynamic thorax phantom used to model respiratory trajectories.

A 3 cm tumor insert was used as target. For each respiratory trajectory, a 3D-CT and 3 repeated 4D-CT scans from random intervals within the respiratory profile were performed on a 4-slice clinical scanner (Lightspeed, GE, WI). Three repeated 4D-CT scans were performed to observe the variation in ITV delineation for different time points within the respiratory trajectory and to obtain the most accurate ITV by taking the average of these three volumes. The Real-time Position Management (RPM system) (Varian, Palo Alto, CA) was used to track the respiratory profiles. The RPM system utilizes an infrared camera and a box with a few reflective markers, which is placed on the abdomen or chest to measure the respiratory pattern and range of motion at the patient surface. This information is modeled as a waveform and used to correlate tumor position to the respiratory cycle. Most importantly, it is used for sorting 4D CT images with different phases.

2.1.2 Contouring and development of new ITV method

The GTV was contoured on the 3DCT, and the ITV was contoured on each of the three MIPs (ITV_{MIP}) generated from the 4DCT. Contouring for all images was done using a consistent lung window by the same person. A volume named ITV_{MIP} was obtained by averaging the three ITV volumes from the MIPs, and this volume was used to represent the typical clinical method of ITV delineation. The new method of creating the ITV to be examined was to combine the GTV and ITV_{MIP}, namely ITV_{COMB}, using the boolean operators in the treatment planning system. The new ITV delineation method was compared to a reference standard, ITV_{RS}, which was obtained by combining all three of the MIP volumes from the 4DCTs. This process of delineating the reference standard ITV essentially encompasses the entire volume captured by the 4DCT.

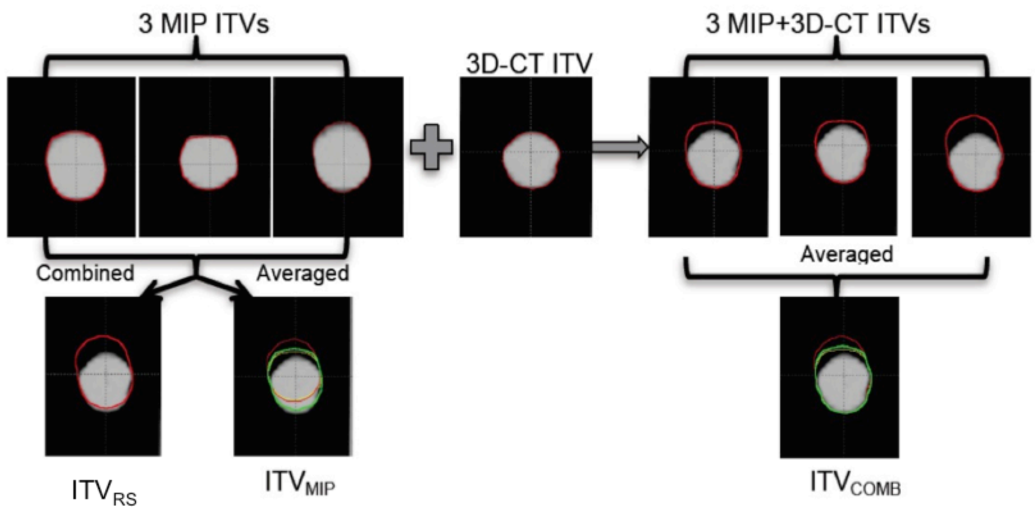

Figure 3: Diagram demonstrating the new process of ITV delineation

2.1.3 Data Analysis

The total volumes for ITV_{COMB}, ITV_{MIP}, and ITV_{RS} were measured in the treatment planning system for all five respiratory trajectories and all three 4DCT scans. The average volumes for ITV_{COMB} and ITV_{MIP} were calculated from the three data sets for each respiratory trajectory. To evaluate which ITV is more accurate, ITV_{COMB} and ITV_{MIP} were compared by calculating the percent error from the reference standard, ITV_{RS}. A two-tailed t-test was performed to determine whether the results were statistically significant.

2.2 Uncertainties in target localization in lung SBRT

To examine CBCT-based target localization errors, the 4D-XCAT digital phantom was used to generate 10-phase 4DCT and CBCT images using in-house developed simulation programs. Images were generated using the same clinical-based parameters as described below for various respiratory profiles (one regular sinusoidal and 10 irregular) and tumor sizes (1 cm, 2 cm, 3 cm). The MIPs and AIPs were generated from the 4DCT datasets. The ITVs were contoured by the same user with the same window/level in the treatment planning system. Image registrations were performed between CBCT and AIP images by matching the target as in the clinic, for each respiratory profile and tumor size.

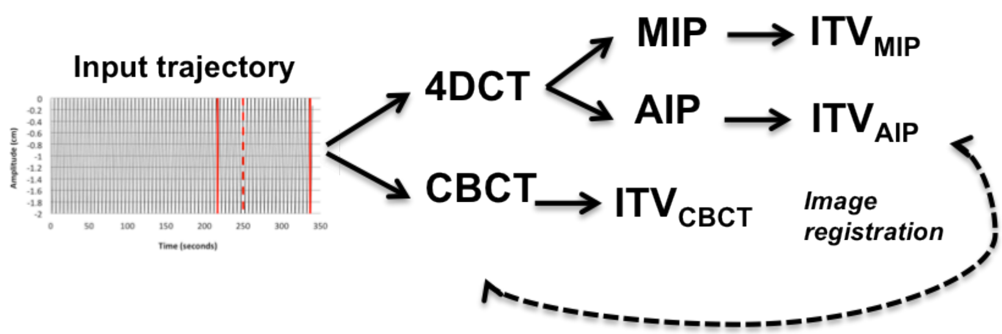

Figure 4: Schematic illustrating overall workflow for the study.

Error of registration was determined as the difference between the manual CBCT-to-AIP registration and the known registration between the two. Correlation between image registration error and respiratory trajectory irregularity was examined.

2.2.1 The XCAT Phantom

For this study, the 4D-XCAT digital phantom was used to generate the 4DCT and CBCT images. The 4D- XCAT phantom is a computer model based on human anatomy and physiology data sets from the National Library of Science's 3D Visible Human project. The 4D-XCAT phantom employs non-uniform rational b-splines or NURBS surfaces, which allow for easy adjustment to the anatomy, enabling realistic patient simulation.

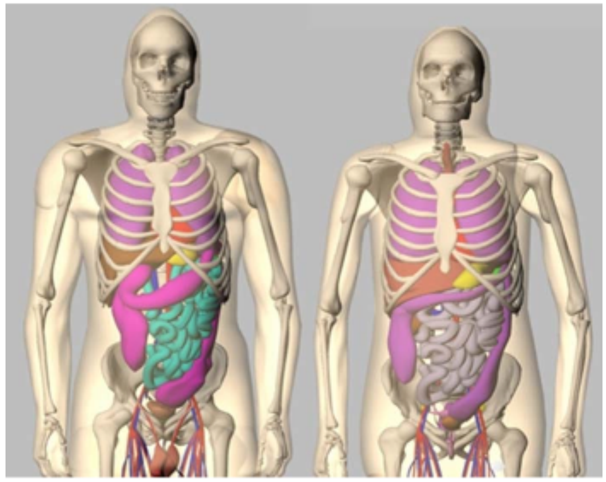

Figure 5: Anterior views of the 4D-XCAT phantoms. (Male- left, Female- right) Illustration courtesy of Dr. William Paul Segars.

The generation of images using the 4D-XCAT phantom is done by a simple CT projection algorithm which given projection geometry information (such as parallel, fan-beam, or cone-beam, distance from the center of the patient to the source, field of view (FOV), and array size), calculates the projection ray intersections through the surface. (15)The 4D-XCAT phantom has the ability to simulate both 3D and 4DCT data.

The 4D-XCAT phantom models respiratory motion based on twenty human 4DCT datasets obtained from Massachusetts General Hospital. Respiratory structures were segmented and made into polygonal models that were visually analyzed on how they changed over the breathing cycle. Motion was assessed for the body, ribcage, lungs, diaphragm, and liver. This patient data was used to determine a general trend in motion for the structures and more accurately represent organ motion during respiration. This trend in motion is modeled by two time curves, one which controls anterior/posterior chest expansion and one which controls changes in diaphragm height. The anterior/posterior chest expansion curve controls ribcage rotation and expansion and forward motion of the diaphragm. The diaphragm height curve controls the contraction of the diaphragm and also the heart, liver, stomach, spleen, and kidney motion. The time curves can be manipulated by the user; for this study, diaphragm motion was set to 2 cm, which models normal breathing behavior. The maximum AP chest expansion was set to 0.5 cm. The motion of the previously mentioned organs and the ribcage are used to set up a motion vector field by voxelizing the thorax of the 4D-XCAT anatomy and assigning integers to each structure. Organs with clearly defined motion are assigned a fixed vector, static organs are set to zero, and additional voxels in the body are initially assigned zero vectors. These motion vector fields are applied to control points and help to define the motion of other organs during respiration. (16)

The 4D-XCAT phantom's ability to reproduce patient respiratory trajectories has been validated. As previously discussed, respiratory mechanics of the 4D-XCAT phantom are controlled by two curves: Tumor motion in three orthogonal directions: superior/inferior, anterior/posterior, and medial/lateral can be controlled to follow any specified motion trajectories or just follow the motion of the lungs. Motion trajectories of the diaphragm, chest, and tumor were obtained from previously acquired MRI scans of 7 subjects and were imported into the 4D-XCAT phantom. (17-22) Isotropic XCAT images of 1mm voxel size were then generated to follow the input motion trajectories. The comparison on input and measured trajectories can be seen in Figure 2 below. The overall mean (± standard deviation) difference in motion amplitude between the input and the measured trajectories is 0.6 (± 0.4) mm, which shows that the 4D-XCAT phantom can accurately reproduce respiratory trajectories. (23)

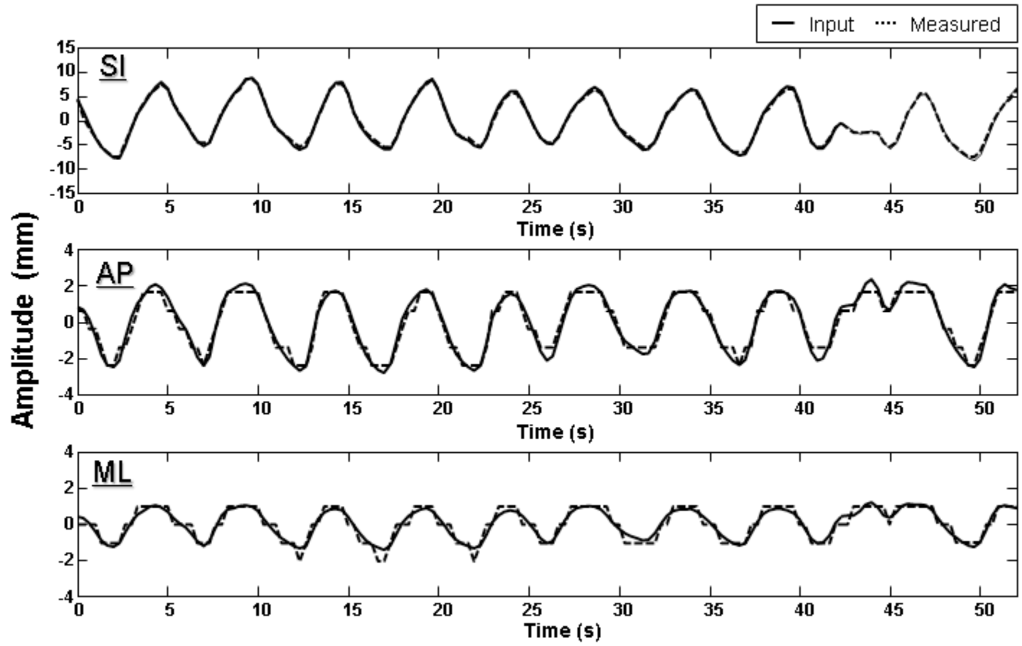

Figure 6: Comparison of input and measured respiratory trajectories.

2.2.2 Data generation

In this study, the FOV was chosen to include the thorax, and a tumor was placed inside the right lung. The tumor parameters were set equally for all trajectories: same location, shape (spherical), and density (equal to water). The size was varied using 1 cm, 2 cm, and 3 cm tumors, which reflect typical lung tumor sizes seen in the clinical setting. The 4D-XCAT MATLAB graphical user interface (GUI) used to generate images can be seen below.

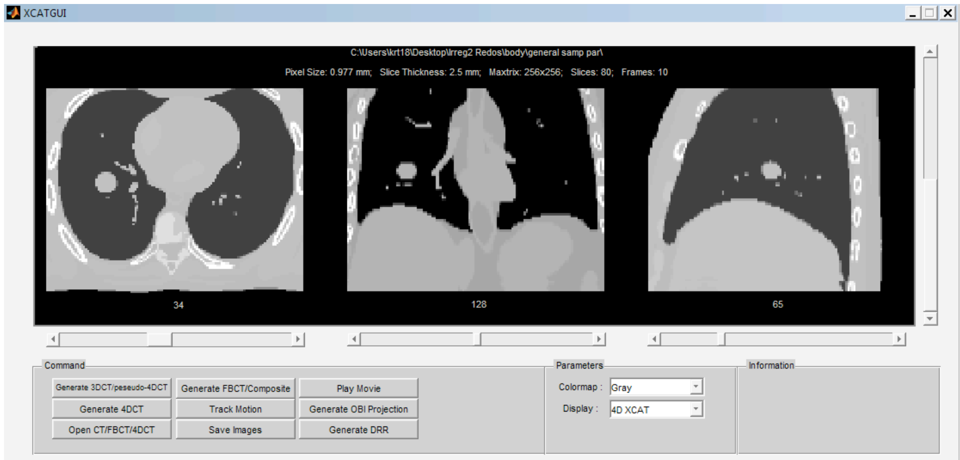

Figure 7: 4D-XCAT graphical user interface used to generate images

A regular respiratory trajectory and irregular respiratory trajectories, illustrated in Appendix A, were used to generate a 4DCT and CBCT for tumor sizes of 1 cm, 2 cm, and 3 cm. The first solid red line denote the start time of the 4DCT and the CBCT, while the second solid red line denotes the end of the 4DCT. The end of the CBCT scan is marked with a dashed red line. The respiratory trajectories were chosen from real patient data recorded on Varian's Real-time Position Management device (RPM) (Varian Medical Systems, Palo Alto, CA). Trajectories that appeared to deviate strongly from a regular sinusoidal curve shape were chosen to be investigated to observe maximum error for patients with irregular breathing.

The respiratory motion modeled was simulated in the superior/inferior direction, with varying amplitude changes. The irregular respiratory trajectories had a mean motion range (±SD) of 0.89 ± 0.25 cm, with values ranging from 0.48 to 1.37 cm. These motion range values are typical of actual patients as observed during lung SBRT treatments at Duke University. Table 1 shows the characteristics of the respiratory profiles chosen to generate the data, including variability of the profile, which will be discussed later in the methods and materials section.

Table 1: Characteristics of respiratory profiles used to generate 4DCT and CBCT data

Profile	Mean motion range (cm)	Max. motion range (cm)	Measure of variability
Regular	1.91	2.00	0
#**1**	0.79	1.43	0.32
#**2**	0.48	1.09	0.48
#**3**	0.80	1.25	0.22
#**4**	1.37	2.00	0.13
#**5**	0.66	1.02	0.24
#**6**	0.81	1.77	0.30
#**7**	1.05	1.39	0.12
#**8**	0.82	1.22	0.22
#**9**	1.05	1.30	0.07
#**10**	1.07	2.00	0.21

The 4DCTs and CBCTs were generated by the XCAT phantom using the same parameters, chosen to be consistent with clinical acquisition parameters, and the tumor position was the consistent for all trajectories. Additionally, the same start time for both scans was also used to eliminate any baseline shifts. The start and end time for the CBCT and 4DCT are denoted on the respiratory trajectories illustrated in the appendix.

2.2.2.1 4DCT Parameters

When generating the 4DCT, CT slices were binned into 10 phases, with 0% as peak inspiration and 50% as peak expiration. The CT acquisition settings were 4 slices per couch position and a cine duration time of 6 seconds. The time between couch positions was assumed to be 0 seconds, as major motion artifacts tend to be introduce in XCAT generated images when a clinical time is used. Images were acquired with 2.5

mm slice thickness and a 0.98 mm resolution, comparable to clinical data, with a 256 x 256 reconstruction matrix. An example 4DCT image, binned into 10 phases is seen in the figure below.

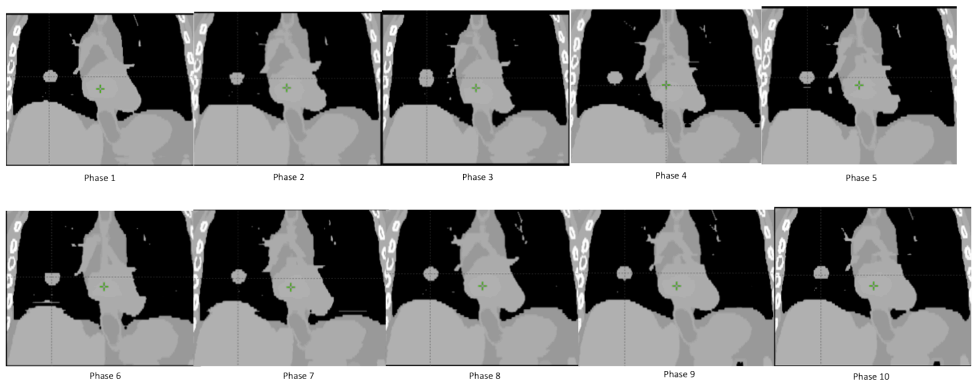

Figure 8: Image illustrating 10-phase 4DCT generated using the 4D-XCAT phantom

2.2.2.2 CBCT Parameters

For the CBCT generation, the tube voltage was 140 kVp, the tube current was 2 mAs per projection, and a 24 degree half-fan angle was used. The CBCT was acquired over 199.2 degrees, with the gantry rotation speed as 6 degrees per second. Each projection acquired every 0.6 degrees, resulting in 333 projections per scan. As with the 4DCT, the slice thickness was 2.5 mm and the slice resolution was 0.98 mm. The CBCT projections were reconstructed using reconstruction matrix size of 256 x 256 and a reconstructed with a feldkamp (FDK) filtered backprojection algorithm. (24) An example of a CBCT generated using the 4D-XCAT phantom is seen below.

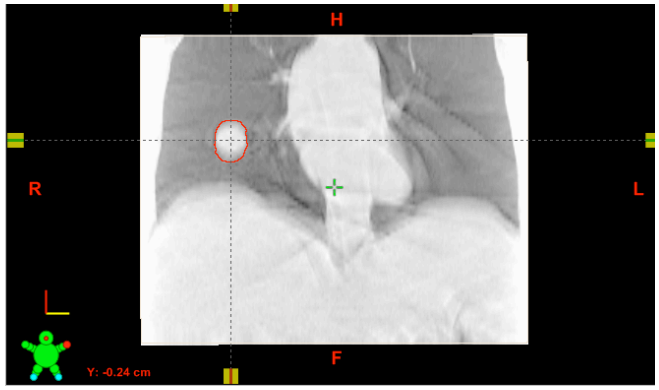

Figure 9: Example of CBCT generated using the 4D-XCAT phantom.

2.2.3 Contouring

The AIP was generated from the 4DCT to be used for contouring. The AIPs for the various respiratory profiles and tumor sizes were contoured in the treatment planning system (Eclipse, Varian Medical Systems, Palo Alto, CA) by the same user with a consistent window and level. To contour the ITV, a volume of interest was selected around the tumor and the CT ranger function was utilized, along with post-processing. The user contouring made any additional cleanup or small changes to the volume subjectively. The planning target volume (PTV) was created using a 3 mm margin from the ITV.

2.2.4 Image Registration

Two different image registrations were performed for the datasets, using the CBCT as the source image and the AIP as the target image. First, a known registration was performed based on differences in coordinate systems when generating the CBCT and 4DCT images. The known translational shifts for the two datasets were 0 mm, 0 mm, 60 mm, in the medial-lateral (ML), anterior-posterior (AP), and superior-inferior (SI) direction, respectively. When generating the CBCT projections, the center was set to 158.75 mm, and the slice thickness was set to 2.5 mm, which equals 63.5 slices, plus one additional slice for starting from one instead of zero. This comes to a total of 64.5 slices for the CBCT. For the 4DCT, 80 slices were generated, with the center being at 40.5. The difference between the CBCT and 4DCT would be 24 slices, which is equal to 60 mm with 2.5 mm slice thickness, explaining the 60 mm shift in the SI direction. Next, a manual PTV-based registration was performed, again using only translational shifts. Four clinicians (two physicists and two radiation oncologists) with expertise in lung SBRT performed the target matching registration to measure the inter-observer variation. A total of 132 image registrations were performed: 4 clinicians performed 33 registrations each. The figure below shows an example of CBCT to- AIP image registration based on target volume matching.

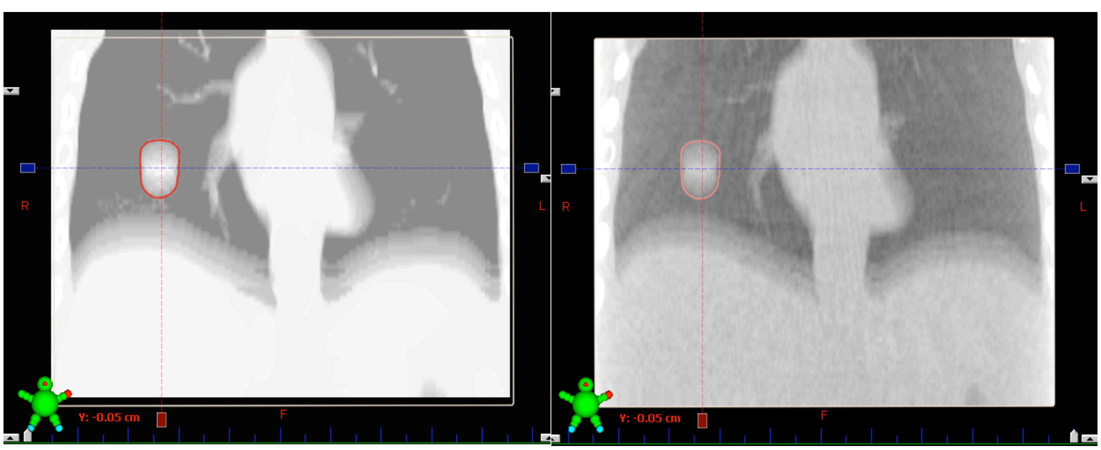

Figure 10: Screenshot illustrating image registration between the AIP (left) and CBCT (right) based on target volume matching.

2.2.5 Data Analysis

The translational shifts between the known registration and the PTV-based registrations for multiple users were subtracted to calculate the relative error in target localization for each respiratory trajectory and corresponding tumor size. The median (± standard deviation) error of CBCT-based registration was reported for each tumor size set and for all tumor sizes combined. Additionally, the variability of each respiratory trajectory was calculated using the following equation:

$$Variability = \frac{\sigma(Peak\,values) + \sigma(Valley\,values)}{2 * mean\,motion\,range}$$

The variability for the full respiratory trajectory and just the portion of the respiratory trajectory used for CBCT generation was calculated. The partial variability from the CBCT respiratory trajectory was chosen for use, as it better represents the variability related to image registration. A correlation study was performed to analyze the relationship between CBCT-based target localization with breathing irregularity and tumor size.

2.3 Examining differences in ITV delineation for MIP, AIP, and CBCT

Using the same data generated for the image registration study using the 4D-XCAT phantom, volume differences in ITV delineation for MIP, AIP, and CBCT were investigated. The ITV was contoured on each dataset by the same user. The MIPs and AIPs were contoured using the same window and level setting and the CT ranger function as previously described. For ITV delineation on the CBCT, the window/level setting was adjusted for optimal target visibility, but kept consistent for all CBCT scans. The volume for the MIP, AIP, and CBCT was measured for each respiratory trajectory and 1 cm, 2 cm, and 3 cm tumor sizes.

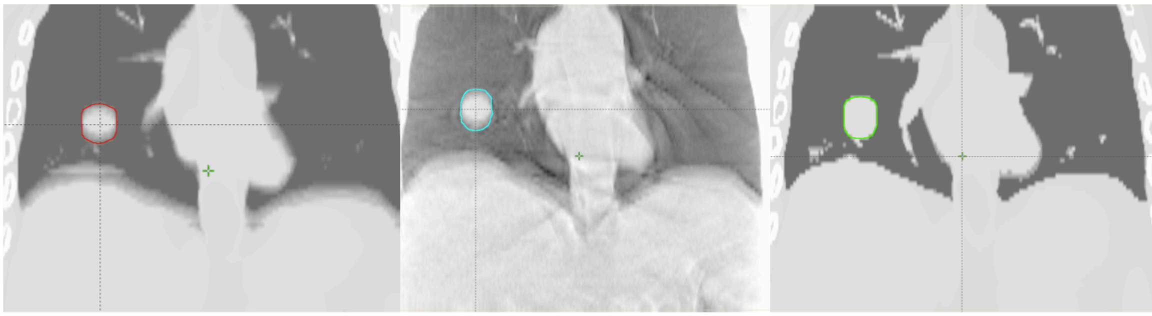

Figure 11: Screenshot illustrating ITV contours for the AIP (red), CBCT (blue), and MIP (green).

Volumes between images were compared and trends corresponding to respiratory variability were examined.

3. Results

Results for the new ITV delineation method, the image registration between CBCT and AIP, and differences observed in ITV for MIP, AIP, and CBCT are discussed below. Results demonstrate that irregular breathing has a notable effect on target delineation, which will further affect setup accuracy in lung SBRT cases. For the ITV delineation study, the mean difference in volume was observed to be significantly different for the two methods. For the image registration study, variability in breathing was seen to increase linearly with increased error in registration. Additionally, fairly large differences in volumes for MIP, AIP, and CBCT-based ITV delineation were observed

3.1 Uncertainties in 4DCT-based ITV delineation

When examining the ITV delineation for the regular profile, both ITV_{MIP} (27.25 cm^3) and ITV_{COMB} (28.12cm^3) were comparable to ITV_{RS} (27.25 cm^3), as expected. This method has been shown to be accurate for sinusoidal, regular respiratory trajectories. However, for irregular profiles, the mean difference between ITV_{COMB} and ITV_{RS} (6.3%±4.9) was significantly (p-value=0.0078) smaller than that between ITV_{MIP} and ITV_{RS} (18.1%±12.3), demonstrating improved accuracy in ITV delineation for the new method. Results for the ITV volumes for the reference standard, typical method, and new method of delineation are seen in Figure 6 below for irregular profiles (#1-4) and the regular sinusoidal profile (#5).

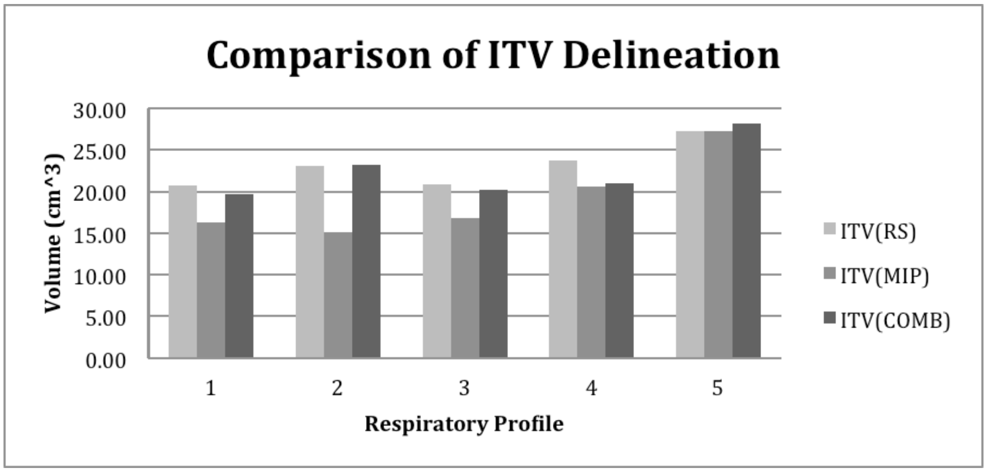

Figure 12: Comparison of ITV volumes to the reference standard as delineated by the typical MIP-based method and the new MIP and GTV-based method. Profiles #1-4 are irregular, and profile #5 is a regular sinusoidal curve.

Additionally, it can be observed that for the irregular respiratory profiles, the ITV delineated on the MIPs from three randomly generated 4DCTs varies. The standard deviation among the three ITVs ranged from 0.04 to 2.94 cm^3, demonstrating the effect that irregular breathing at different time points of the respiratory trajectory can affect the volume of the ITV.

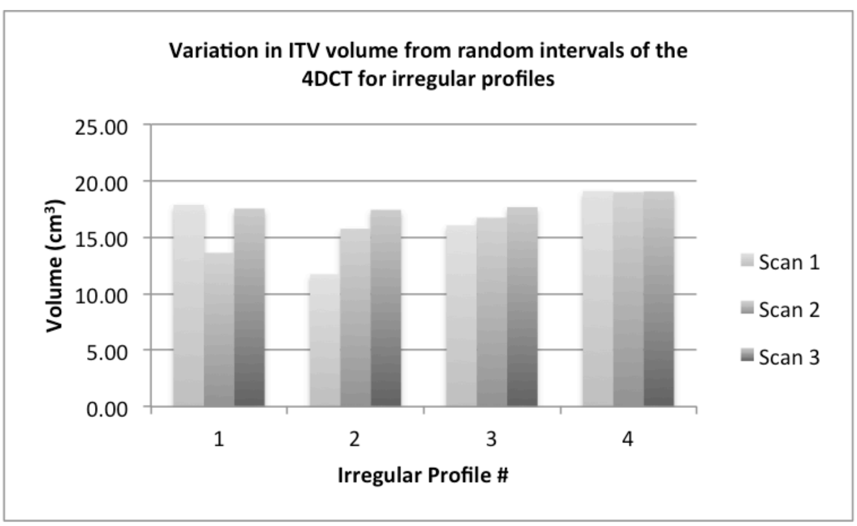

Figure 13: Variation in ITV from three randomly generated 4DCTs for irregular respiratory profiles.

3.2 Target localization accuracy in lung SBRT

It has already been shown that respiratory variability affects delineation of the ITV, but it also affects another important step in the treatment process: image registration. CBCT-to-AIP registration based on the PTV was examined for one regular profile and ten irregular profiles, for different tumor sizes. Results below support the hypothesis that respiratory variability does affect accurate image registration, and therefore will affect the treatment accuracy for lung SBRT cases.

3.2.1 Overall results observed for target localization error

As expected, negligible errors of registration (median ≤ 0.5 mm) were found for the regular respiratory profile for all tumor sizes: the median (± SD) error was 0.50 (± 0.73) mm, 0.20 (± 0.17) mm, and 0.40 (± 0.22) mm in the medial-lateral (ML), anterior-posterior (AP), and superior-inferior (SI) direction, respectively. For the irregular profiles and all tumor sizes, small errors (median=0.5 mm) were found in the ML and AP directions, while non-trivial errors were seen in the SI direction (median (±SD): 1.90 (±1.55) mm). Maximum error of registration for the irregular profiles in the ML, AP, and SI direction was 1.0 mm, 2.0 mm, and 5.4 mm, respectively. Figure 5 shows the errors of registration for each profile.

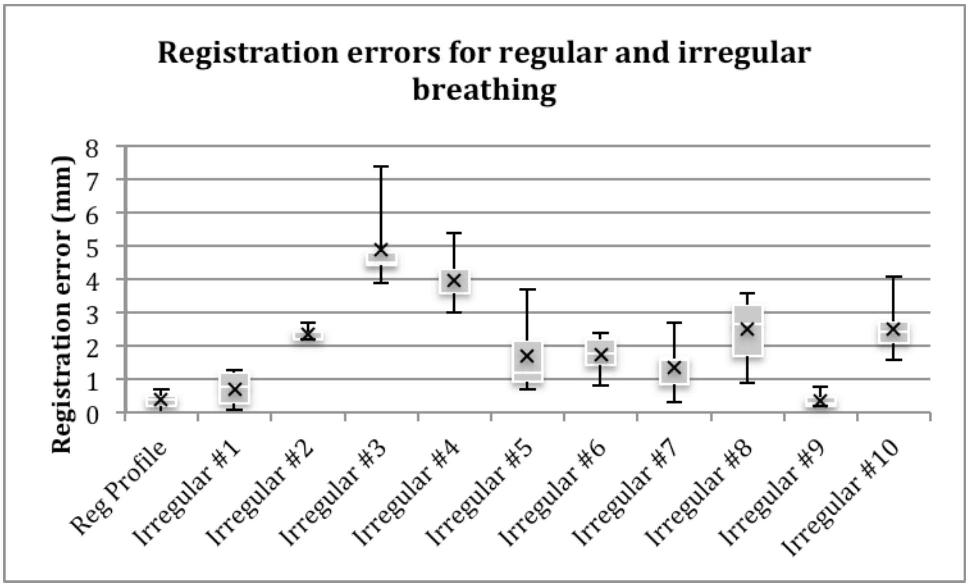

Figure 14: Boxplot of image registration errors for various respiratory trajectories.

The inter-observer variability was investigated, and the SD of registration error among observers was 0.15 mm, 0.34 mm, and 0.69 mm, in the ML, AP, and SI directions, respectively, which were all smaller than their respective mean error or registration. This eliminates the concern that error in image registration is dependent on individual methods and style of image registration. Results showed a linear trend between respiratory variability and median error in image registration for all tumor sizes combined and individually grouped tumor sizes.

3.2.2 Difference in error among different tumor size groups

For grouped tumor sizes, the mean (± SD) error was observed to decrease with increasing tumor size: 2.45 (± 1.68 mm), 2.19 (± 1.45 mm), and 1.97 (± 1.52 mm) for 1 cm, 2 cm, and 3 cm tumor sizes, respectively. An analysis of variance (ANOVA) test was performed, which is comparable to a t-test except it tests the means of more than two groups. Results of the ANOVA test showed no significant difference in mean error of registration for different tumor size groups ($p>0.6$). The error in registration among different tumor size groups is illustrated in the figure below.

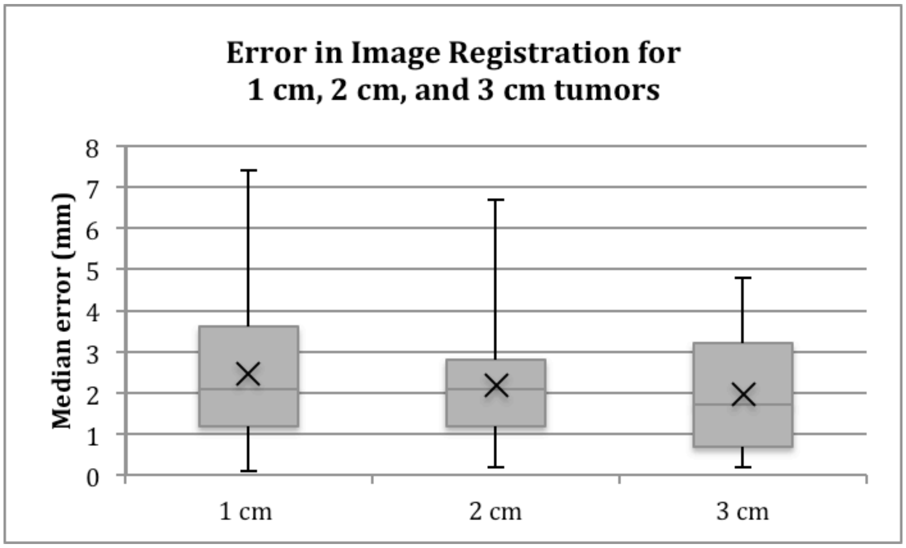

Figure 15: Illustration of error in image registration among different tumor size groups.

It can also be observed that the larger the tumor size, the smaller the variation in registration of error.

3.2.3 Correlation between error in the S/I direction and respiratory variability

When observing the relationship between respiratory variability and image registration in the SI direction, a mild linear trend can be observed. However, no direct correlation was observed between error of registration error and breathing irregularity for all tumor sizes combined and for each tumor size group individually.

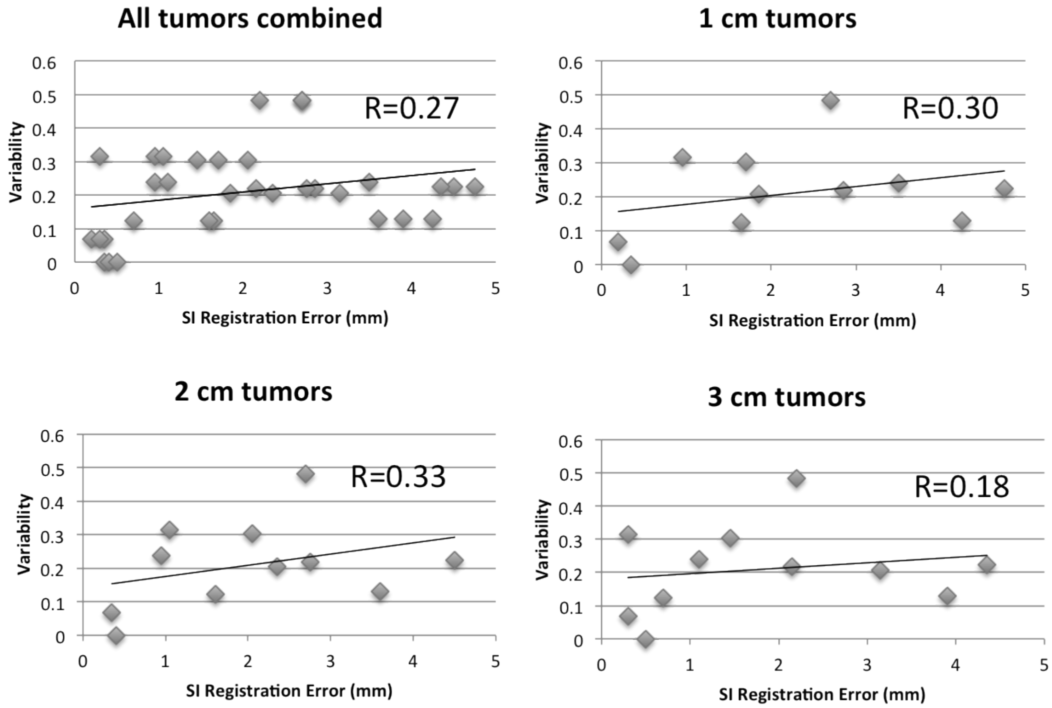

Figure 16: Plots demonstrating correlation between breathing variability in respiratory trajectory and median error in CBCT-to-AIP image registration for all tumor sizes and for each tumor size separately.

When grouping the data into low and high variability groups for all tumor sizes (low variability=0-0.22, high variability=0.22+), it can be seen that for high variability respiratory trajectories, there is a greater median error in the SI direction. This difference was found to be significant ($p<0.001$). Additionally, for high variability respiratory trajectories, there is a greater range in error. When examining the individual tumor size groups, there is again a greater median error for high variability trajectories. However, the range in error is seen to decrease with increasing tumor size, as expected. The difference between high and low variability image registration shifts for individual tumor size groups was not significant (p=0.21, 0.32, and 0.46) for 1 cm, 2 cm, and 3 cm tumor groups, respectively.

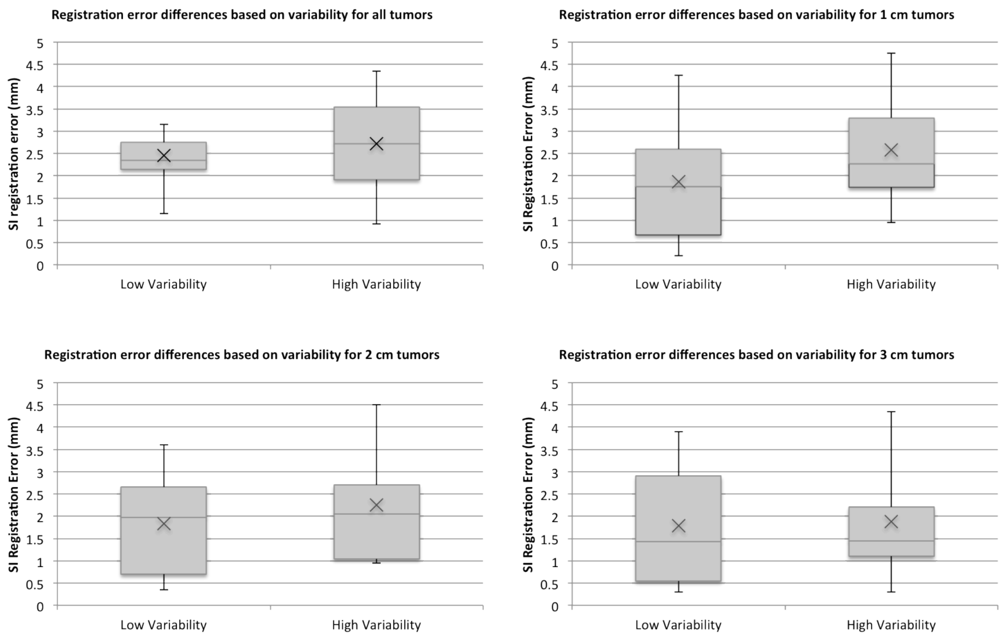

Figure 17: Comparison of median error in the SI direction for low vs. high variability respiratory trajectories for all tumor sizes and individual groups

3.2.4 Correlation between error in the S/I direction and I/E ratio

Additionally the ratio of inspiration to expiration (I/E) was calculated using a ratio of the number of points that were within 25% of the peak inhale and exhale portions of the cycle and averaging over the full respiratory cycle. A table of results for I/E ratios can be seen below.

Table 2: I/E ratios for respiratory profiles

Profile	I/E
Reg	1.12
Irreg1	1.23
Irreg2	1.93
Irreg3	0.84
Irreg4	0.72
Irreg5	0.59
Irreg6	0.23
Irreg7	0.41
Irreg8	0.64
Irreg9	0.39
Irreg10	0.38

The correlation between these I/E ratios and the SI registration error was examined for all tumor sizes combined and for individual tumor size groups, but no correlation was determined. The plots for these results can be seen below.

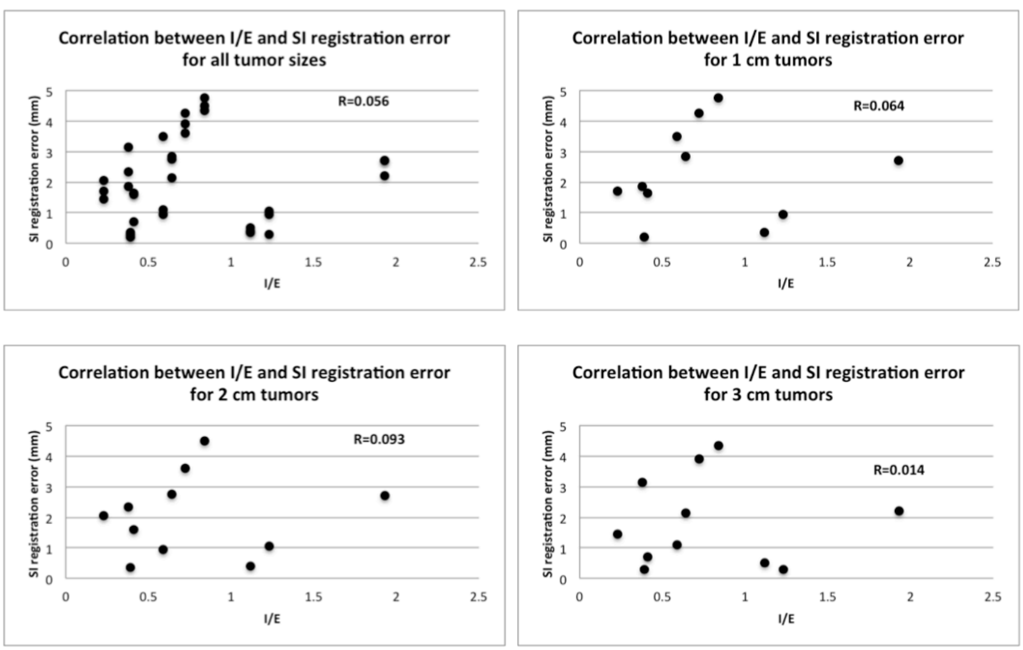

Figure 18: Correlation between SI registration error and inspiration to expiration ratio

3.3 Differences in ITV for MIP, AIP, and CBCT

Differences in ITV delineation for MIP, AIP, and CBCT-based methods were observed and compared. AIP and MIP-based volumes were comparable, however the AIP volumes were slightly smaller. This finding supports the reasoning for using the MIP-based delineation of the ITV in the clinical setting. When comparing the CBCT-based ITV delineation to the MIP and AIP, it was found that the volume was even more underestimated, as illustrated in the figures below for each tumor size group.

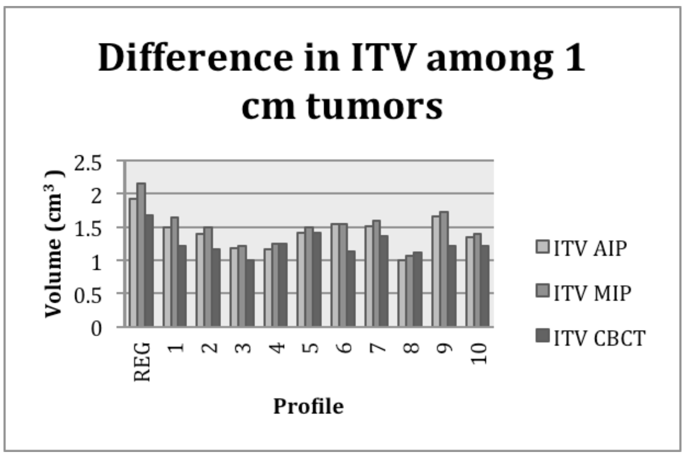

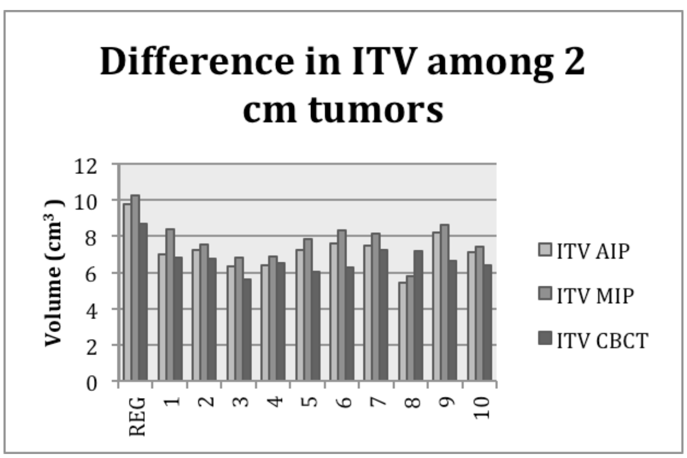

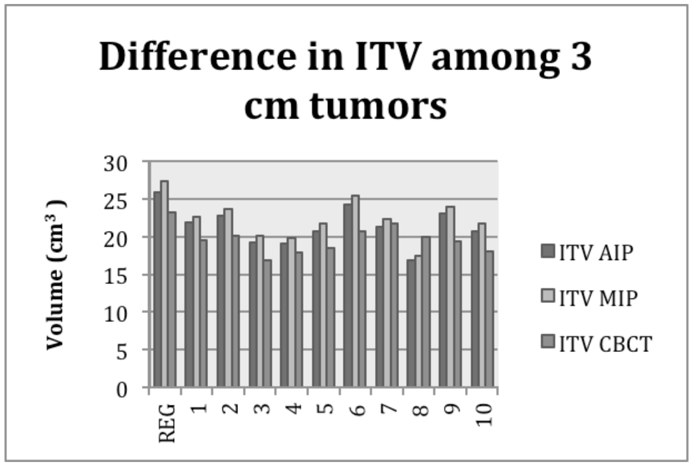

Figure 19: Plots demonstrating difference in volumes of MIP, AIP, and CBCT-based ITV delineation for 1 cm, 2 cm, and 3 cm tumors.

For the 1 cm tumors the mean (±SD) ITV volumes were 1.42 (±0.25) cm^3, 1.51 (±0.29) cm^3, and1.25 (±0.18) cm^3 for the AIP, MIP, and CBCT, respectively. For the 2 cm tumors the mean (±SD) ITV volumes were 7.25 (±1.11) cm^3, 7.82 (±1.16) cm^3, and 6.74 (±0.80) cm^3 for the AIP, MIP, and CBCT, respectively. For the 3 cm tumors the mean (±SD) ITV volumes were 21.43 (±2.53) cm^3, 22.38 (±2.72) cm^3, and 19.65 (±1.84) cm^3 for the AIP, MIP, and CBCT, respectively.

When comparing the different ITV delineation methods, the largest percent error occurs between the MIP and CBCT-based methods for all tumor sizes and is seen to decrease with increasing tumor size. The smallest percent error is seen between the MIP and AIP-based ITV delineation methods, which is expected since they are generated form the same 4DCT dataset. Percent errors for different methods and tumor sizes can be seen in the table below.

Table 3: Average percent error for ITV delineation methods among different tumor size groups

	MIP-AIP	MIP-CBCT	AIP-CBCT
1 cm tumors	5.7%	17.8%	12.2%
2 cm tumors	7.6%	14.4%	6.8%
3 cm tumors	4.3%	12.7%	8.4%

The differences between ITV volumes delineated on the AIP and MIP for each tumor size group were not significant (p=0.47, 0.25, and 0.41 for 1 cm, 2 cm, and 3 cm tumor sizes respectively). For 1 cm, 2 cm, and 3 cm tumor groups, the difference in ITV volume between MIP and CBCT was significant in all cases (p=0.011, 0.010, 0.006). The difference between CBCT and AIP ITV volume was significant for the 1 cm and 3 cm tumor groups (p=0.041 and 0.036), and found to be not significant for the 2 cm group (p=0.116). For all tumor sizes grouped together, the difference between AIP-MIP, MIP-CBCT, and CBCT-AIP, was not significant (p=0.81, 0.26, 0.69). Correlation between breathing irregularity and difference in volume of MIP ITV and CBCT ITV was examined. No notable correlation was observed.

4. Discussion

Results for each of the portions of this study demonstrate that irregular breathing has an effect on ITV delineation and image registration in lung SBRT. A new method for ITV delineation which encompasses a larger portion of the target volume has been investigated and proven that its results are significantly different from the typical method of ITV delineation. Differences in ITV volumes for MIP, AIP, and CBCT images were examined, and it was shown that the current delineation method for all of these types of images may deviate from the true value due to breathing irregularity. Finally, image registration for irregular respiration can further induce error in the process.

4.1 Limitations of this study

This study limits itself to one spherical tumor shape, density, and one tumor position within the lung. Realistically, lung SBRT patients have varying tumor shapes, sizes, and locations, so further examination could be made into the image artifacts generated from non-spherical tumors at varying positions and irregular respiratory trajectories. Liu et al. found that tumor location has a significant impact on ITV delineation from CBCT versus 4DCT; tumors near the center of the lung had a high CT background which reduced contrast of the tumor at the edges, making it difficult to accurately delineate the ITV. Tumors in the center compared to tumors near the periphery of the lung significantly underestimated the ITV in the CBCT ($p=0.046$). (13) The impact that irregular respiration has on tumors near the center versus the periphery should be examined.

Additionally, only translational setup shifts were considered, disabling the ability in the treatment planning system for rotational shifts. This study also used the same 4DCT and CBCT image acquisition parameters as used in the Duke University clinic, including slice thickness, gantry rotation speed, and half-fan beam angle for CBCT. Therefore, the findings of this project are limited to images acquired using the same parameters. Additionally, the 4DCT and CBCT for each respiratory trajectory were generated at the same starting time to eliminate baseline shifts. For actual patients, this obviously would not be the case. Therefore, it is possible that further error would be induced by randomly selecting the starting time within the respiratory trajectory as in a clinical setting. This is especially the case for irregular respiratory profiles that drift.

4.2 Clinical impact

For the examined new method of ITV delineation, the results suggest that combining the V of the 3D-CT with the ITV of the MIP is more accurate than the ITV of the MIP alone, and thus would be a simple method to reduce breathing irregularity induced errors in ITV delineation for treatment planning of lung cancer. This process would require additional contouring time from the physician, so it may not be feasible to implement in the clinic. However, it could be argued that the improved accuracy for ITV delineation is worth the additional contouring time to ensure that patients receive as accurate of a treatment as possible.

Other studies have examined the effect of the ratio of inspiration to expiration (I/E) on ITV delineation on the CBCT. Vergalasova et al. reported that an I/E ratio of less than one limits the ability to represent the full extent of target motion. This effect was seen to increase with decreasing I/E ratios. The study made the conclusion that this target volume underestimation could impact the patient alignment and planning if a center-to-center registration technique is used. (14) The I/E ratios for the respiratory trajectories used in this project could be examined in a further study to see how they affect the target volume and image registration error, but no correlation was observed.

When examining the results from the image registration error study, it can be observed that the error in the SI direction is non-trivial (median (±SD): 1.90 (±1.55) mm and maximum: 5.40 mm). The PTV margin for lung SBRT is typically 3-5 mm, but this includes patient setup error on the table only. When you consider an additional margin for image registration error, it is likely that greater error on the order of 1 cm is induced. Because target localization accuracy is of extreme importance in lung SBRT, this additional error poses a further layer of uncertainty for treatment accuracy. It is important to note that the motion simulated in this study was in the SI direction, with variations in amplitudes only.

The main concern for target localization accuracy in lung SBRT treatments is that the errors in setup will be further carried out through treatment and affect the efficacy of treatment. Studies have been done to analyze how irregular breathing affects dosimetric accuracy in treatment planning for lung SBRT. Huang et al. found that for irregular breathing with movement ranges greater than 2 cm, the measured isodose lines were shifted in comparison to the treatment plan. Additionally, they concluded that the inaccuracies between planned and delivered dose could be attributed to erroneous depiction of target motion in the 4DCT, which indicates that this study is clinically relevant for patients with irregular breathing. (25)

4.3 Other relevant studies

The sample size in this study was limited due to the amount of time required for data generation. Generation of data for additional irregular respiratory trajectories and tumor sizes could demonstrate a stronger correlation between registration error and variability. The patient-positioning error for lung SBRT cases could also be further examined using 4D-CBCT to evaluate whether a reduction in error occurs based on improved image quality. Additionally, a cost-benefit analysis could be performed to determine whether this reduction in positioning error is worth the extra time and dose that the patient would receive, as well as the risk that the patient would move during the longer scan. Sweeney et al. showed that target localization for 3D-CBCT compared to 4D-CBCT was significantly worse and that tumor positions differed by 3.6 mm ± 3.2 mm on average for 3D-CBCT and 1.9 mm ± 0.9 mm using 4D-CBCT. (26) Further investigation of this concept could lead to an additional correlation study.

Clements et al. conducted a similar studying, analyzing the effect of respiratory variability on MIP to CBCT registration errors using a respiratory motion phantom modeling four computer-generated respiratory trajectories and six patient RPM respiratory trajectories. Their study used a center-to-center ITV registration technique and examined differences in length of the ITV. A trend in MIP ITV volume reduction was seen for respiratory trajectories with increasing amplitude, and volumes were reduced up to 20% compared to the true ITV. The study also found that CBCT ITV volumes were even further reduced by up to 30%, which coincides with the findings in this study. Overall, findings for MIP to CBCT based image registration were comparable to our findings for AIP and CBCT based image registration. (27)

5. Conclusion

It has been shown that the typical MIP-based method for ITV delineation underestimates the target volume. The results of this study suggest that combining V of the 3D-CT with the ITV of the MIP is more accurate than the ITV of the MIP alone, and thus would be a simple method to reduce breathing irregularity induced errors in ITV delineation for treatment planning of lung cancer. Large differences among ITV volumes for MIP, AIP, and CBCT were also observed, reinforcing the concept that accurate delineation has a large dependence on the type of image that's being contoured.

Additionally, it has been demonstrated that CBCT-to-AIP image registration in lung SBRT patients with irregular breathing can be erroneous, especially in the superior-inferior direction. The error is largely induced by breathing irregularity and could not be overcome by perfecting manual matching.. Uncertainties in target matching should be considered when determining the ITV to PTV margin.

Appendix A: Illustrations of RPM respiratory trajectories

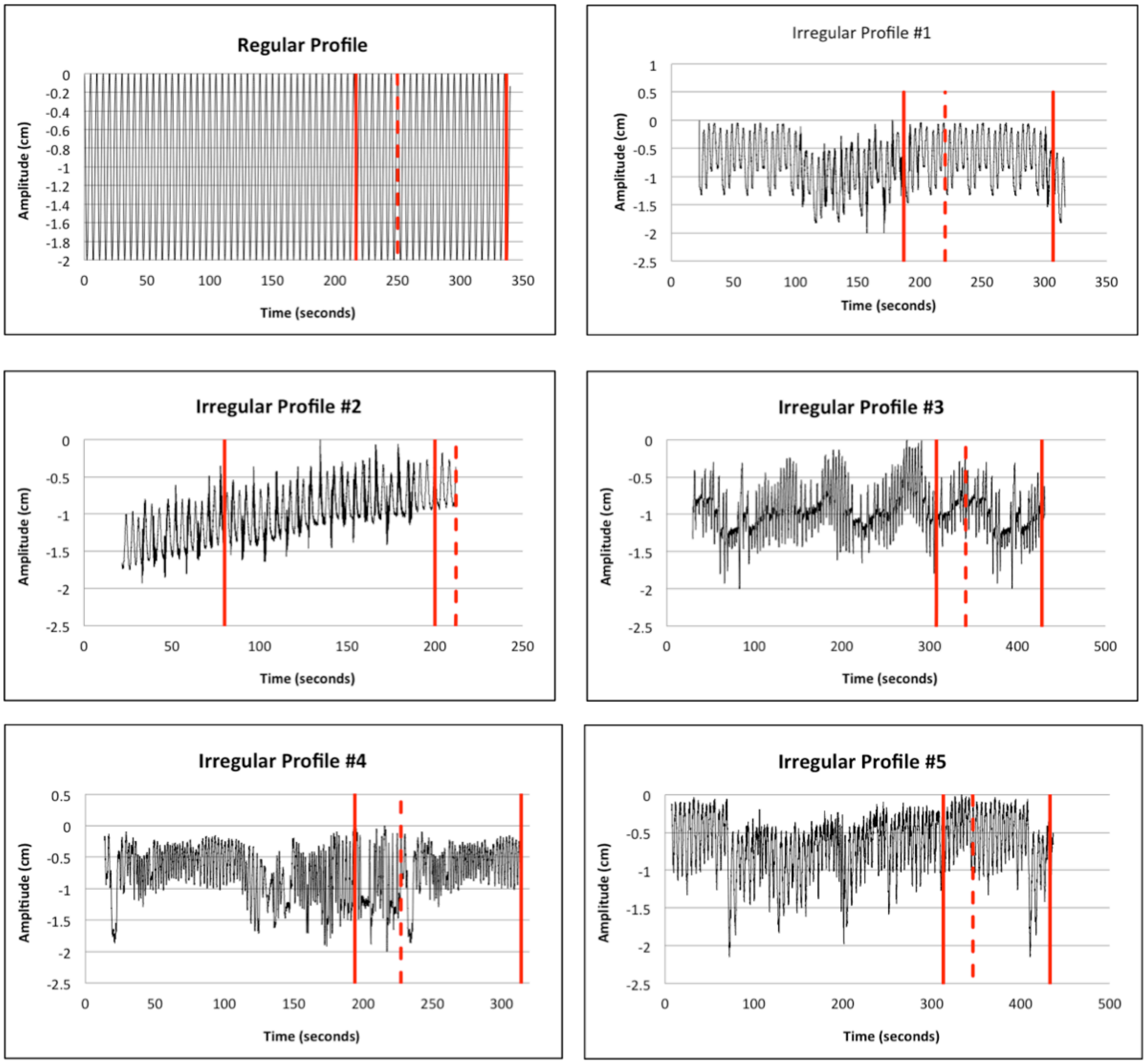

The first solid red line denote the start time of the 4DCT and the CBCT, while the second solid red line denotes the end of the 4DCT. The end of the CBCT scan is marked with a dashed red line.

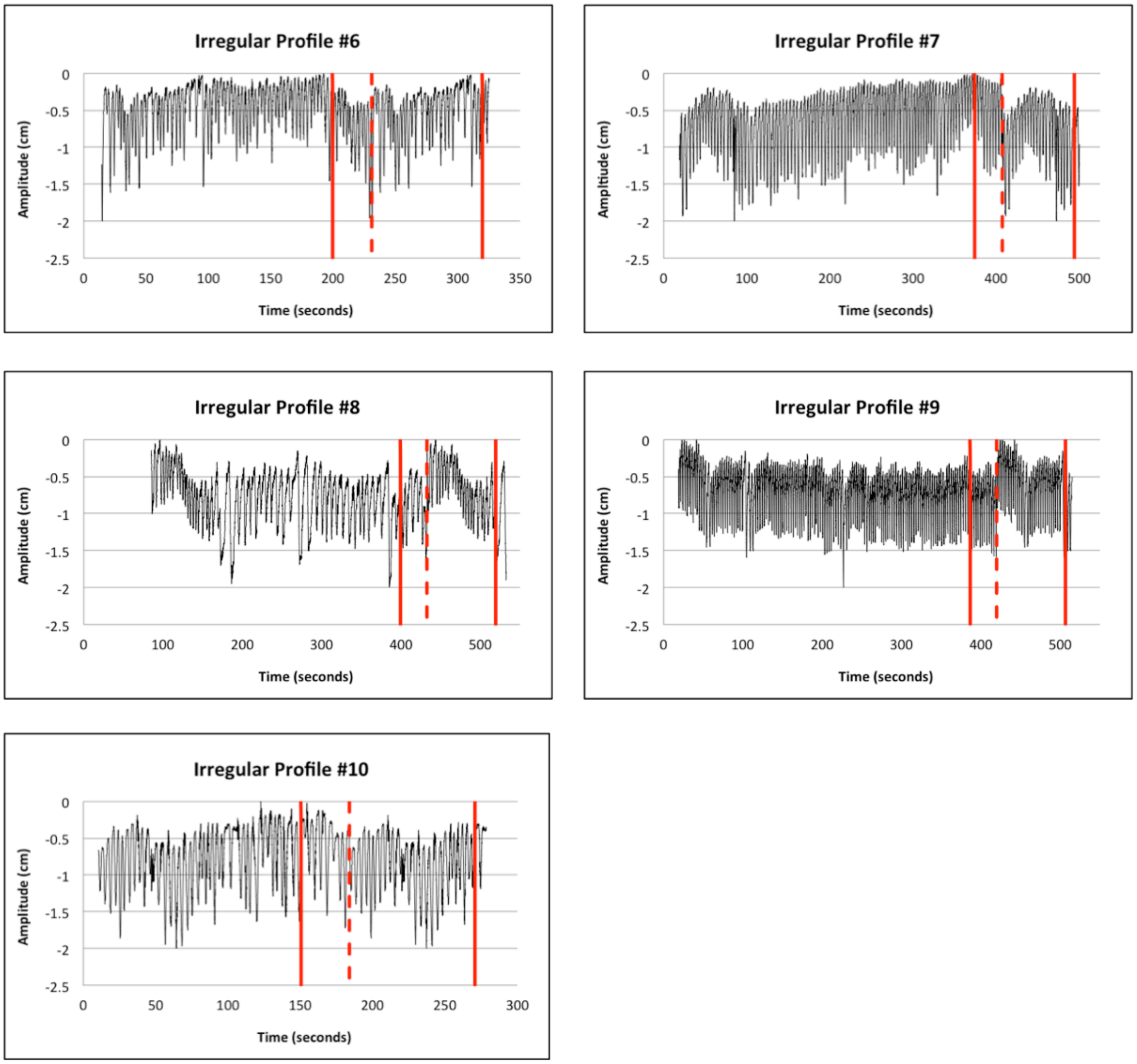

The first solid red line denote the start time of the 4DCT and the CBCT, while the second solid red line denotes the end of the 4DCT. The end of the CBCT scan is marked with a dashed red line.

References

1. U.S. Cancer Statistics Working Group. *United states cancer statistics: 1999–2009 incidence and mortality web-based report*. Atlanta: U.S. Department of Health and Human Services, Centers for Disease Control and Prevention and National Cancer Institute; 2013.

2. Timmerman R, Papiez L, McGarry R, Likes L, DesRosiers C, Frost S, et al. Extracranial stereotactic radioablation: Results of a phase I study in medically inoperable stage I non-small cell lung cancer. Chest. 2003 Nov;124(5):1946-55.

3. Duncker-Rohr V, Nestle U, Momm F, Prokic V, Heinemann F, Mix M, et al. Stereotactic ablative radiotherapy for small lung tumors with a moderate dose. favorable results and low toxicity. Strahlenther Onkol. 2013 Jan;189(1):33-40.

4. Nguyen NP, Garland L, Welsh J, Hamilton R, Cohen D, Vinh-Hung V. Can stereotactic fractionated radiation therapy become the standard of care for early stage non-small cell lung carcinoma. Cancer Treat Rev. 2008 Dec;34(8):719-27.

5. Dahele M, Pearson S, Purdie T, Bissonnette JP, Franks K, Brade A, et al. Practical considerations arising from the implementation of lung stereotactic body radiation therapy (SBRT) at a comprehensive cancer center. J Thorac Oncol. 2008 Nov;3(11):1332-41.

6. Rietzel E, Pan T, Chen GT. Four-dimensional computed tomography: Image formation and clinical protocol. Med Phys. 2005 Apr;32(4):874-89.

7. Yamamoto T, Langner U, Loo BW,Jr, Shen J, Keall PJ. Retrospective analysis of artifacts in four-dimensional CT images of 50 abdominal and thoracic radiotherapy patients. Int J Radiat Oncol Biol Phys. 2008 Nov 15;72(4):1250-8.

8. Mutaf YD, Antolak JA, Brinkmann DH. The impact of temporal inaccuracies on 4DCT image quality. Med Phys. 2007 May;34(5):1615-22.

9. Sarker J, Chu A, Mui K, Wolfgang JA, Hirsch AE, Chen GT, et al. Variations in tumor size and position due to irregular breathing in 4D-CT: A simulation study. Med Phys. 2010 Mar;37(3):1254-60.

10. Sonke JJ, Zijp L, Remeijer P, van Herk M. Respiratory correlated cone beam CT. Med Phys. 2005 Apr;32(4):1176-86.

11. Li T, Schreibmann E, Yang Y, Xing L. Motion correction for improved target localization with on-board cone-beam computed tomography. Phys Med Biol. 2006 Jan 21;51(2):253-67.

12. James SS, Mishra P, Hacker F, Berbeco RI, Lewis JH. Quantifying ITV instabilities arising from 4DCT: A simulation study using patient data. Phys Med Biol. 2012 Mar 7;57(5):L1-7.

13. Liu HW, Khan R, D'Ambrosi R, Krobutschek K, Nugent Z, Lau H. The influence of target and patient characteristics on the volume obtained from cone beam CT in lung stereotactic body radiation therapy. Radiother Oncol. 2013 Feb 7.

14. Vergalasova I, Maurer J, Yin FF. Potential underestimation of the internal target volume (ITV) from free-breathing CBCT. Med Phys. 2011 Aug;38(8):4689-99.

15. Segars WP, Mahesh M, Beck TJ, Frey EC, Tsui BM. Realistic CT simulation using the 4D XCAT phantom. Med Phys. 2008 Aug;35(8):3800-8.

16. Segars WP, Mori S, Chen GTY, Tsui BMW. Modeling respiratory motion variations in the
4D NCAT phantom. IEEE Nuclear Science Symposium Conference Record. In press 2007.

17. Cai J, Read PW, Baisden JM, Larner JM, Benedict SH, Sheng K. Estimation of error in maximal intensity projection-based internal target volume of lung tumors: A simulation and comparison study using dynamic magnetic resonance imaging. Int J Radiat Oncol Biol Phys. 2007 Nov 1;69(3):895-902.

18. Cai J, Read PW, Sheng K. The effect of respiratory motion variability and tumor size on the accuracy of average intensity projection from four-dimensional computed tomography: An investigation based on dynamic MRI. Med Phys. 2008 Nov;35(11):4974-81.

19. Cai J, McLawhorn R, Read PW, Larner JM, Yin FF, Benedict SH, et al. Effects of breathing variation on gating window internal target volume in respiratory gated radiation therapy. Med Phys. 2010 Aug;37(8):3927-34.

20. Cai J, Read PW, Larner JM, Jones DR, Benedict SH, Sheng K. Reproducibility of interfraction lung motion probability distribution function using dynamic MRI: Statistical analysis. Int J Radiat Oncol Biol Phys. 2008 Nov 15;72(4):1228-35.

21. Cai J, Read PW, Altes TA, Molloy JA, Brookeman JR, Sheng K. Evaluation of the reproducibility of lung motion probability distribution function (PDF) using dynamic MRI. Phys Med Biol. 2007 Jan 21;52(2):365-73.

22. Cai J, Sheng K, Sheehan JP, Benedict SH, Larner JM, Read PW. Evaluation of thoracic spinal cord motion using dynamic MRI. Radiother Oncol. 2007 Sep;84(3):279-82.

23. Panta RK, Segars P, Yin FF, Cai J. Establishing a framework to implement 4D XCAT phantom for 4D radiotherapy research. J Cancer Res Ther. 2012 Oct;8(4):565-70.

24. Feldkamp L, Davis L, and Kress J. Practical cone-beam algorithm. J. Opt. Soc. Am. A. 1984;1:612-619.

25. Huang L, Park K, Boike T, Lee P, Papiez L, Solberg T, et al. A study on the dosimetric accuracy of treatment planning for stereotactic body radiation therapy of lung cancer using average and maximum intensity projection images. Radiother Oncol. 2010 Jul;96(1):48-54.

26. Sweeney RA, Seubert B, Stark S, Homann V, Muller G, Flentje M, et al. Accuracy and inter-observer variability of 3D versus 4D cone-beam CT based image-guidance in SBRT for lung tumors. Radiat Oncol. 2012 Jun 8;7:81,717X-7-81.

27. Clements N, Kron T, Franich R, Dunn L, Roxby P, Aarons Y, et al. The effect of irregular breathing patterns on internal target volumes in four-dimensional CT and cone-beam CT images in the context of stereotactic lung radiotherapy. Med Phys. 2013 Feb;40(2):021904.